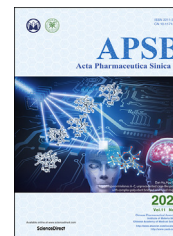




Chinese Pharmaceutical Association
Institute of Materia Medica, Chinese Academy of Medical Sciences

Acta Pharmaceutica Sinica B

www.elsevier.com/locate/apsb
www.sciencedirect.com



ORIGINAL ARTICLE

Protocatechuic aldehyde protects cardiomyocytes against ischemic injury via regulation of nuclear pyruvate kinase M2



Xunxun Wu^a, Lian Liu^a, Qiuling Zheng^b, Haiping Hao^{a,b}, Hui Ye^{a,c,*},
Ping Li^{a,*}, Hua Yang^{a,*}

^aState Key Laboratory of Natural Medicines, China Pharmaceutical University, Nanjing 210009, China

^bCollege of Pharmacy, China Pharmaceutical University, Nanjing 210009, China

^cJiangsu Provincial Key Laboratory of Drug Metabolism and Pharmacokinetics, China Pharmaceutical University, Nanjing 210009, China

Received 3 December 2020; received in revised form 14 January 2021; accepted 10 February 2021

KEY WORDS

Protocatechuic aldehyde;
PKM2;
 β -Catenin;
TCF4;
Heart ischemia;
Myocardial infarction;
Apoptosis;
Mitochondrial damage;
Nuclear translocation

Abstract Rescuing cells from stress damage emerges a potential therapeutic strategy to combat myocardial infarction. Protocatechuic aldehyde (PCA) is a major phenolic acid in Chinese herb Danshen (*Salvia miltiorrhiza* root). This study investigated whether PCA regulated nuclear pyruvate kinase isoform M2 (PKM2) function to protect cardiomyocytes. In rats subjected to isoprenaline, PCA attenuated heart injury and protected cardiomyocytes from apoptosis. Through DARTS and CETSA assays, we identified that PCA bound and promoted PKM2 nuclear translocation in cardiomyocytes exposed to oxygen/glucose deprivation (OGD). In the nucleus, PCA increased the binding of PKM2 to β -catenin via preserving PKM2 acetylation, and the complex, in cooperation with T-cell factor 4 (TCF4), was required for transcriptional induction of genes encoding anti-apoptotic proteins, contributing to rescuing cardiomyocyte survival. In addition, PCA ameliorated mitochondrial dysfunction and prevented mitochondrial apoptosis dependent on PKM2. Consistently, PCA increased the binding of PKM2 to β -catenin, improved heart contractive function, normalized heart structure and attenuated oxidative damage in mice subjected to artery ligation, but the protective effects were lost in *Pkm2*-deficient heart. Together, we showed that PCA regulated nuclear PKM2 function to rescue cardiomyocyte survival via β -catenin/TCF4 signaling cascade, suggesting the potential of pharmacological intervention of PKM2 shuttle to protect the heart.

Abbreviations: CETSA, cellular thermal shift assay; CK-MB, creatine kinase isoenzyme-MB; DARTS, drug affinity responsive target stability; ISO, isoprenaline; LDH, lactate dehydrogenase; NRVMs, neonatal rat ventricular myocytes; OGD, oxygen and glucose deprivation; PCA, protocatechuic aldehyde; PKM2, pyruvate kinase isoform M2; ROS, reactive oxygen species; shRNA, short hairpin RNA; TCF4, T-cell factor 4; TUNEL, deoxy-nucleotidyl transferase-mediated dUTP nick end-labeling.

*Corresponding authors.

E-mail addresses: cpuyehui@cpu.edu.cn (Hui Ye), liping2004@126.com (Ping Li), yanghua@cpu.edu.cn (Hua Yang).

Peer review under responsibility of Chinese Pharmaceutical Association and Institute of Materia Medica, Chinese Academy of Medical Sciences.

<https://doi.org/10.1016/j.apsb.2021.03.021>

2211-3835 © 2021 Chinese Pharmaceutical Association and Institute of Materia Medica, Chinese Academy of Medical Sciences. Production and hosting by Elsevier B.V. This is an open access article under the CC BY-NC-ND license (<http://creativecommons.org/licenses/by-nc-nd/4.0/>).

1. Introduction

Myocardial infarction (MI) is a leading cause of global morbidity¹, and cardiomyocyte loss has been proposed as a critical determinant of heart injury. Although nutrient depletion is the direct cause of cell necrosis in the infarct focus, many contributing factors impair cells *via* different mechanisms. Of note, oxidative stress, inflammation and calcium overload converge on mitochondrial dysfunction, resultantly leading to mitochondrial apoptosis, an important way for cell death in ischemic heart². Due to the minimal regenerative capacity of adult mammalian heart^{3–5}, protection of cardiomyocyte survival emerges as an important means to limit ischemic injury.

Accumulating studies have reported the important role of pyruvate kinase isoform M2 (PKM2) in aerobic glycolysis, cell cycle and apoptosis, especially in tumors⁶. Conventionally, PKM2 is known as a rate-limiting glycolytic enzyme that catalyzes the conversion of phosphoenolpyruvate to pyruvate. PKM2 shuttles between the cytosol and the nucleus and functions on a subcellular compartment-dependent manner. In the cytosol, PKM2 exists primarily as an enzymatically active tetramer. Although the formation of PKM2 dimer is enzymatically inactive, it can translocate to the nucleus where it functions as a co-activator for the transcriptional regulation of genes involved in cell proliferation and tumor development^{7,8}. Despite PKM2 is highly expressed in tumor cells, recent studies have revealed its role in heart. High level of PKM2 is associated with reduce apoptosis and oxidative stress in cardiomyocytes exposed to oxygen and glucose deprivation (OGD)⁹. In infarcted myocardium, PKM2, together with hypoxia-inducible factor-1 α (HIF-1 α), has demonstrated a contribution to ATP synthesis *via* glycolysis¹⁰. After heart transplantation, PKM2 expression is also observed to be positive correlated to cardiomyocyte survival¹¹. The adult mammalian heart has limited regenerative capacity; however, PKM2 is demonstrated to regulate postnatal cardiomyocytes cycle and protect cell survival from ischemic insult¹². These events raise the possibility that nuclear PKM2 can increase cardiomyocyte resistance to ischemic injury.

Once entering the nucleus, PKM2 dimer exerts other functions beyond glycolysis¹³. In the nucleus, PKM2 phosphorylates proteins involved in cell growth and survival^{14,15}. β -Catenin is a transcriptional regulator involved in cell proliferation and survival *via* regulation of several genes. Usually, β -catenin is a key effector of WNT signaling in the nucleus, responsible for the control of cell fate *via* regulation of WNT-specific genes¹⁶. In fact, nuclear PKM2 is a multi-tasking regulator, as it interacts with different transcription factors to influence cell fate¹⁶. In cancer cells, upon epidermal growth factor (EGF) stimulation, PKM2 translocates into the nucleus and binds to β -catenin, and this complex is recruited to the promoter region for transcriptional regulation of cell proliferation in a manner that is independent of WNT signaling⁷. β -Catenin reduces myocardial infarct size and protects cardiomyocytes from lipotoxicity-induced apoptosis^{17,18}, indicative of the potential of cardioprotection.

Protocatechuic aldehyde (PCA) is a natural phenolic compound found in Chinese herb Danshen (*Salvia miltiorrhiza* root), which has been widely used for the treatment of cardiovascular diseases, including ischemic damage^{19,20}. By screening a chemical library consisting of 304 natural compounds, we had found that PCA could potentially protect cardiomyocytes from oxidative damage in our previous work¹⁹. As a phenolic acid, the anti-oxidative effects of PCA have been well documented^{21–23}. Although PCA attenuates heart injury against ischemic injury¹⁹, and decreases apoptosis in vessel endothelial and smooth muscle cells from different mechanisms^{24–26}, the exact role in cardioprotection remains to be revealed. Herein, we identified PKM2 as a potent candidate targeted by PCA. Because PKM2 in the nucleus regulates cardiomyocyte cell cycle through β -catenin pathways¹², we invested the role of PCA with a focus on the function of nuclear PKM2. We showed that PCA promoted the nuclear translocation of PKM2, and rescued cardiomyocyte survival *via* β -catenin/T-cell factor 4 (TCF4) signaling cascades in the setting of ischemic injury. These results suggested that pharmacological intervention of PKM2 shuttle is a potential therapeutic strategy to prevent ischemic damage.

2. Materials and methods

2.1. Chemicals and reagents

Protocatechuic aldehyde (purity \geq 98%) was purchased from Yuanye Biotechnology Co., Ltd. (Shanghai, China). PhosSTOP (4906837001) and EDTA-free, EASYpack protease inhibitor (4693116001) were obtained from Roche (Shanghai, China). Pronase (10165921001) and isoprenaline (I5627) were purchased from Sigma–Aldrich (St. Louis, MO, USA). Trypsin (0.25%), protein A/G magnetic beads (Pierce™, 88802) and Mito-Tracker Red FM (M22425) were all obtained from Thermo Fisher Scientific (Shanghai, China). The H2DCFDA (HY-D0940) fluorescence probe was obtained from MCE (Shanghai, China). PNU-74654 (S8429) was obtained from Selleck (Shanghai, China). Antibodies against PKM2 (4053), SIRT6 (12486), cleaved caspase 3 (9664s), α -actinin (6487), mouse anti-rabbit IgG (light-chain specific, D4W3E) mAb (93702) and the rabbit IgG (2729) were purchased from Cell Signaling Technology (Beverly, MA, USA). Antibodies against GAPDH (60004-1-Ig), β -catenin (51067-2-AP, 66379-1-Ig), PCNA (10205-2-AP), caspase 3 (66470-2-Ig), BAX (60267-1-Ig), BCL-2 (60178-1-Ig), PKM2 (60268-1-Ig), β -tubulin (10068-1-AP) and TCF4 (22337-1-AP) were obtained from Proteintech (Wuhan, China). Annexin V-FITC apoptosis detection Kit was obtained from Beyotime (C1062M, Suzhou, China).

2.2. Animals and treatments

Male Sprague–Dawley rats at 7–8-week old (200–220 g) were obtained from Shanghai Sippr-BK laboratory animal Co., Ltd. (Shanghai, China), while male C57BL/6 mice at 4–8 weeks were obtained from comparative medical center of Yangzhou University (Yangzhou, China). Animals were housed in a constant

temperature (20 ± 2 °C) and a 12-h light/dark cycle. All animal studies were performed under the authorization of the animal ethics committee of China Pharmaceutical University (Nanjing, China).

The isoprenaline (ISO)-induced myocardial damage rats model was established by subcutaneous (sc) injection of ISO (65 mg/kg with an one-day interval for 2 consecutive days) as described previously²⁷ and PCA (20 and 40 mg/kg) was orally administrated after the first injection for consecutive 5 days. Then, rats were euthanized for the collection of the heart. The level of lactate dehydrogenase (LDH) and creatine kinase isoenzyme-MB (CK-MB) in the blood were determined using commercial kits (CK12, DOJINDO Laboratories, Shanghai, China; CSB-E14403r, Cusabio, Wuhan, China).

For the permanent coronary ligation mice model, in brief, mice were anesthetized with sodium pentobarbital (50 mg/kg, i.p.). Following tracheal intubation, the left thoracotomy was opened. Then, a left anterior descending (LAD) coronary artery occlusion was performed. Mice in the sham group undergone the same surgical procedures except ligation. Then, PCA (80 mg/kg) was orally administrated to mice for 3 weeks and the echocardiography (Vevo 3100LT micro-ultrasound system, Visual Sonics Inc., Toronto, Ontario, Canada) was examined. In brief, mice were anesthetized and the echocardiography of the left ventricle was obtained. The left ventricular function parameters such as ejection fraction (EF) and fractional shortening (FS) were recorded according to the M-mode images acquired. The contents of 8-hydroxydeoxy guanosine levels (8-OHdG, ab201734) and lipid peroxidation (4-HNE, ab238538) in the heart were measured by commercial kits. Myocardial infarction area of mice hearts was determined using Image J software (NIH Image, Bethesda, MD, USA).

For *Pkm2*-knockdown (KD) in the heart of mice, the adeno-associated virus (AAV) delivery system was selected to deliver AAV9-cTNT-GFP-sh*PKM2* for cardiac *Pkm2*-KD mice and deliver scrambled shRNA for the control group. The mice were injected with 200 μ L of virus containing 4×10^{11} AAV9 *via* the tail vein. Western blotting analysis for PKM2 and green fluorescent protein (GFP) was conducted to confirm the PKM2 knock-down efficiency.

2.3. Preparation of primary neonatal rat ventricular myocytes (NRVMs) and cell culture

NRVMs were harvested from Sprague–Dawley rats (1–2-day-old, Shanghai Sippr-BK laboratory animal Co., Ltd., Shanghai, China). The hearts were collected and cut into pieces, followed by digestion with 0.5% type II collagenase (Worthington, USA) in a 37 °C water bath for 8–10 times. Next, the cells were collected after centrifugation at $3000 \times g$, room temperature for 15 min (5430R, Eppendorf, Hamburg, Germany) and cultured in DMEM containing 10% of fetal bovine serum (10270–106, FBS, Gibco, USA) for 2 h. In order to increase the purity of cardiomyocytes, a differential adhesion method was adopted, and then cells were cultured in DMEM (10% FBS) supplemented with 200 μ mol/L BrdU to restrain the proliferation of fibroblast. NRVMs grown to the third or fourth day with a marked beat were used for experiments.

H9C2 cell line was obtained from Cell Bank of the Chinese Academy of Sciences (Shanghai, China) and cultured in DMEM (KeyGEN Biotech, Nanjing, China) supplemented with 10% FBS in humidified 5% CO₂ at 37 °C.

To specifically knock down *Pkm2* expression in NRVMs, *Pkm2* short hairpin RNA (shRNA) or scrambled (NC) shRNA were transfected using Lipofectamine® 3000 transfection reagent (Invitrogen, L3000008, USA). The shRNA sequence was listed in Supporting Information Table S1.

2.4. Cell survival and oxidative indexes analysis

NRVMs were incubated in glucose-free DMEM under 1% O₂ or stimulated with 100 μ mol/L H₂O₂ in the presence of PCA at given concentrations. Cell viability was determined by the assay using commercial CCK-8 kits (Dojindo Laboratories, Kumamoto, Japan). Cell apoptosis in the heart was assayed with an *in situ* apoptosis detection kit based on the terminal deoxynucleotidyl transferase-mediated TUNEL (Beyotime, Suzhou, China). Caspase 3 activity and pyruvate kinase activity were determined by commercial kits (C1116, Beyotime; K709-100, Biovision).

Intracellular reactive oxygen species (ROS) were stained with cell permeable DCFH-DA fluorescent probe and determined by a microplate reader.

2.5. Drug affinity-responsive target stabilization assay (DARTS)

The DARTS assay was conducted according to literature with minor modifications^{28,29} in H9C2 cells. In brief, approximately 1×10^7 untreated H9C2 cells were lysed with a mammalian protein extraction reagent (#78501, Thermo Scientific) on ice for 30 min. Indicated concentrations of PCA (diluted in $1 \times$ TNC buffer, 50 mmol/L Tris, 50 mmol/L NaCl, 10 mmol/L CaCl₂, pH = 7.4) was supplement into the aliquoted cell lysate (500 μ g total protein, 5 μ g/ μ L). Then, to allow sufficient ligand–protein target binding, samples were gently mixed followed by incubation for 2 h at room temperature. Aliquoted lysates were then digested by pronase at a 1:500 ratio (*w/w*) for precisely 30 min. Then, loading buffer was added into the lysates and boiling for 10 min. The resulting samples were separated by sodium dodecyl sulfate polyacrylamide gel electrophoresis (SDS-PAGE) and stained with Coomassie blue.

2.6. Mass spectrometry analysis

Upon staining, gel bands with significant abundance changes following PCA incubation were noted at about ~ 60 kD. This band was excised, destained, reduced, alkylated and digested by trypsin (Promega, Madison, WI, USA). Then, the digest was extracted and desalted on a C18 Ziptip (Millipore, Milford, MA, USA). After that, vacuum dried and reconstituted was performed. An online nanoUPLC system Acquity (Shimadzu, Japan) coupled to a Triple TOF™ 5600 mass spectrometer (SCIEX, Framingham, MA, USA) was used for LC–MS/MS analysis. A trapping column (ChromXP C18, 3 μ m, 120 Å, 350 μ m i.d. 0.5 mm, Eksigent) and an analytical column (ChromXP C18, 3 μ m, 120 Å, 15 cm, Eksigent) were employed. Mobile phases A [0.1% (*v/v*) formic acid in water] and mobile phase B [0.1% (*v/v*) formic acid in acetonitrile] were used in this study. A 60-min-length gradients of 1%–40% mobile phase B (300 nL/min) was used for separation. For MS acquisition, the full MS scan range was set to *m/z* 350–1500 (scan time: 0.2 s). The mass error tolerance was set at 30 ppm and 0.15 Da, respectively. The raw data was processed by PEAKS Studio (BSI Solutions, Waterloo, CA, USA) and searched against the rattus uniprot database (<http://www.uniprot.org/>).

2.7. Recombinant PKM2 protein

The open reading frames (ORFs) for *Pkm2* (NM_001378868.1) were codon-optimized, synthesized (Sangon Biotech, Shanghai, China), cloned into a pET28a vector and transformed into *E. coli* BL21 (DE3) competent cells. Monoclonal strains were selected and cultured in LB medium containing kanamycin (75 µg/mL) at 37 °C in shaking flasks until the optical density at 600 nm reaching 0.6 to 0.8. Next, the cells were induced with 0.1 mmol/L isopropyl β-D-thiogalactoside (IPTG) at 16 °C for 24 h, and then harvested the supernatant for PKM2 purification. The PKM2 protein was purified using a His-tag Protein Purification Kit (P2226, Beyotime, Suzhou, China).

2.8. Cellular thermal shift assay (CETSA)

For cell lysate CETSA experiments, H9C2 cells were lysed with a freeze–thawed method using liquid nitrogen. The resultant cell lysates were then divided into two fractions, one incubated with the solvent as the control group and the other incubated with PCA (100 µmol/L) for 30 min at room temperature as the PCA-treated group. Then, the two groups of lysates were aliquoted, respectively, followed by heating at sequentially increased temperature (39–66 °C with a 3 °C interval). After heating, the lysates were centrifuged (12,000×g, 10 min, 4 °C; 5430R, Eppendorf, Hamburg, Germany) and PKM2 abundance level in the supernatants was analyzed by immunoblotting.

For the living cell CETSA experiments³⁰, H9C2 cells were pre-treated with PCA (100 µmol/L) for 2 h, and then cells were heated for 3 min at indicated temperatures followed by cooling at room temperature. After that, cells were collected and 100 µL protein loading buffer was added followed by boiling for 10 min. Then, lysates were assayed by immunoblotting against PKM2.

2.9. Surface plasmon resonance (SPR) assay

Interaction between PCA and PKM2 was quantitatively measured using the Biacore T200 system (GE Healthcare Life Sciences, Uppsala, Sweden). Purified recombinant PKM2 protein was immobilized on a carboxymethylated 5 (CM5) sensor chip. Gradient concentrations of PCA (1.25–20 nmol/L) were injected as analytes. Data were analyzed using a Biacore evaluation software (T200 Version 2.0).

2.10. Immunoblotting experiments

Treatment cells were lysed with RIPA lysis buffer (P0013D, Beyotime, Suzhou, China) supplemented with protease inhibitor cocktail on ice. Then, to normalization of assayed samples, a BCA assay (P0010, Beyotime) was performed. Then, cell lysates were separated by SDS-PAGE gel and transferred onto nitrocellulose membrane. After blocking with 5% non-fat milk for 1 h, the membrane was incubated with indicated primary-antibody solution overnight at 4 °C. The next day, the membrane was washed for three times followed by incubation with horse radish peroxidase (HRP)-conjugated secondary antibodies for 2 h at room temperature. After washing, resulting bands were detected using an Azure C600 system (Azure Biosystems, CA, USA), and the relative quantification of bands was analyzed *via* Image J software.

For co-immunoprecipitation assay, lysates were centrifuged (12,000×g, 10 min, 4 °C), and the resulting supernatants were

collected. After measuring the protein concentrations using the BCA assay kit (Beyotime), a 200 µg protein was transferred and incubated with 2 µL IgG or the primary antibodies on a rotator for 4 °C overnight. Then, 30 µL protein A/G magnetic agarose beads (Pierce #78609, USA) were added and allowed to incubate with the lysates for another 4 h. Subsequently, the beads were washed with the NP-40 buffer for 4 times. After that, 100 µL of 1 × SDS-PAGE loading buffer was added to the pellet and boiling for 10 min.

2.11. Molecular docking

The protein structure used in this study for docking analysis was downloaded from the protein data bank (PDB ID 1t5a). The leDock software (<http://lephar.com>)³¹ was employed to generate an ensemble of docked conformations for PCA bound to PKM2. Crystal water and FBP were removed, and hydrogen atoms were added. PCA was then docked into PKM2 on the basis of evolutionary optimization of the ligand pose. The binding site of PCA was defined as proteinaceous residues located within a distance of 4 Å radius from PCA.

2.12. Immunofluorescence analysis

NRVMs were seeded in cell dish and fixed with 4% paraformaldehyde solution for 30 min. After washing for three times, cells were incubated in 5% FBS (0.3% Triton X-100) for 1 h at room temperature. Immunofluorescent staining was performed with primary antibody (anti-PKM2, anti-α-actinin) overnight at 4 °C. After incubation with secondary antibodies (Alexa Fluor® 594, ab150116) for 1 h, cells were incubated with DAPI (Abcam, ab104139) for 5 min at room temperature. Then, a DeltaVision Ultra microscopic imaging system was selected for cell imaging (GE Life Science, Boston, MA, USA).

2.13. The assay of mitochondrial permeability transition pore (mPTP) and mitochondrial fission

After treatment, mPTP was detected with Mitochondrial Permeability Transition Pore Assay Kit (C2009S, Beyotime). The fluorescent intensities of mPTP were analyzed using Image J software. For mitochondrial fission assay, treated NRVMs were washed with PBS and incubated with 50 nmol/L Mito Tracker Red CMXRos (M22425, Thermo Fisher Scientific, San Jose, CA, USA) for 30 min at 37 °C. The fluorescence intensities were determined at the single cell level on a DeltaVision Ultra microscopic imaging system (GE Life Science, Boston, MA, USA). The mitochondrial fission results were determined by the percentage of cells undergoing mitochondrial fission from 6 cells in three independent experiments.

2.14. Luciferase reporter assay and quantitative real-time PCR

NRVMs were seeded at a density of 5000 cells per well in 96-well plates, incubated for 24 h, and then transfected with TCF/LEF1 luciferase reporter plasmid. At 24 h post-transfection, cells were treated with PCA for 4 h, and then lysed with lysis buffer for 30 min. Firefly luciferase activities was determined from lysates using luciferase assay system (Vazyme Biotech, China) in a Berthold TriStar² SLB929 modular monochromator multimode reader (Berthold Technologies, Germany).

For quantitative real-time PCR, heart tissues or cells were firstly isolated (R401-1, Vazyme Biotech) and reverse transcribed (R223-1, Vazyme Biotech) using commerce reagent according to the manufacturer's instructions. Then, quantitative real-time PCR experiment (Q121-1, Vazyme Biotech) was performed using the LightCycler 480 q-PCR system (Roche Molecular Systems, Inc., Basel, Switzerland). The primer sequences used in this paper were listed in Supporting Information Table S2.

2.15. Histological analysis

Slices of hearts were fixed in 4% paraformaldehyde, dehydrated and embedded in paraffin. Heart sections (5 μm -thick) were stained with hematoxylin and eosin (HE) and masson for histopathological evaluation. The protein expression of cleaved caspase 3, BAX and BCL-2 were measured by immunohistochemistry (IHC) staining. Cross-sectional area of cardiomyocytes was determined using Image J software.

2.16. Statistical analysis

The between-group variances were similar, and the data were normally distributed. The comparisons between groups (>2 two groups) were performed using one-way ANOVA (Tukey's multiple comparisons test). Significance between two groups was performed by Student's two-tailed *t* test with GraphPad Prism 6.01 (Graphpad Software, San Diego, CA, USA). All data are represented as mean \pm SD, unless otherwise specified.

3. Results

3.1. PCA protects the heart against ischemic injury

We first observed the effects of PCA on cardioprotection in rats subjected to isoprenaline (ISO) insult (Supporting Information Fig. S1A), as persistent β -adrenergic receptor stimulation induces heart injury owing to the convergence of more contributing factors, including oxidative stress, inflammation and thrombosis³². ISO challenge induced heart injury, indicated by the leakage of CK-MB and LDH, which was normalized by oral administration of PCA (20 and 40 mg/kg, 5 days; Fig. 1A and B). PCA administration reduced the ratio of heart weight to tibia length (HW/TL, Fig. 1C). HE staining shows that ISO induced cardiac injury with fiber broken, but PCA administration reduced the cardiac infarct surface and cardiomyocyte cross-sectional area with structure normalization, indicating the potential to attenuate cardiomyocyte hypertrophy (Fig. 1D). PCA administration reduced 4-HNE and 8-OHdG contents in the heart, indicative of the ability to reduce lipid peroxidation and DNA damage (Fig. 1E and F). BAX is a pro-apoptotic protein, while BCL-2 is an anti-apoptotic protein. Immunohistochemistry staining shows that PCA decreased BAX expression with an increase in BCL-2 expression, contributing to reducing the formation of cleaved caspase 3 (Fig. 1G). As expected, PCA prevented cell apoptosis in rat heart subjected to ISO insult (Fig. 1H). In line with this, PCA concentration-dependently rescued cell survival in primary neonatal rat ventricular myocytes (NRVMs) when exposed to oxygen and glucose deprivation (OGD, cells were cultured in glucose-free DMEM under 1% O₂) or H₂O₂ stimulation (Fig. 1I and J). Increased ROS production was also reduced by PCA administration in NRVMs when exposed to OGD (Fig. 1K).

3.2. PCA directly binds to PKM2 in cardiomyocytes

Next, we sought to reveal the molecular mechanism of PCA in cardioprotection. Due to the relatively small and simple structure of PCA (Fig. S1B), we employed a DARTS approach to identify the potential candidates that interact with PCA, because this assay identifies direct targets for the ligand without additional modification^{29,33}. DARTS detects ligand-bound targets in lysates basing on their increased resistance to proteolysis²⁹. For the assay in cell lysates after proteolytic digestion, high concentration of the tested ligand is required to ensure the stability change detectable³³, we incubated PCA with H9C2 cells lysates at concentrations of 100 and 200 $\mu\text{mol/L}$, and found a Coomassie blue-stained band at \sim 60 kD that became more abundant upon PCA incubation, likely due to the resistance to pronase degradation (Fig. 2A). Mass spectrometry analysis was employed to identify candidate proteins targeted by PCA in this specific gel band. Screening of the identified proteins that fall within the expected molecular weight (MW) range conferred PKM2 as a top-ranking protein (Supporting Information Table S3 and Fig. S1C).

PCA binding increased the stability of PKM2, and this action was further confirmed by PKM2 immunoblotting in DARTS-processed H9C2 cell lysates (Fig. 2B). Similarly, incubation with PCA increased the resistance to pronase degradation of the purified recombinant PKM2 (Fig. 2C and Fig. S1D). In addition, the PCA-PKM2 interaction was demonstrated by an orthogonal target validation approach, CETSA. CETSA recognizes ligand-target engagement by immunoblotting detection of increased stability of the target proteins towards heat-induced precipitation. As expected, PCA incubation stabilized PKM2 in heat-denatured H9C2 cell lysates and intact H9C2 cells (Fig. 2D and E). In support, SPR analysis revealed the potential interaction of PCA-PKM2 interaction ($K_D = 5.76$ nmol/L, Fig. 2F). Collectively, these data suggest that PCA directly interacted with PKM2 in cardiomyocytes as well as on a recombinant protein level.

3.3. PCA protects cardiomyocytes dependently on PKM2

Because PCA at a concentration of 10 $\mu\text{mol/L}$ effectively protected cell survival against OGD and H₂O₂ insults (Fig. 1I and J), we used this concentration as a working concentration in the following experiments. As PKM2 was assigned as the potential candidate of PCA, we asked whether the protective effects of PCA was dependent on PKM2. We depleted *Pkm2* gene with short hairpin RNA (shRNA) in NRVMs, and this treatment did not impair cell survival (Supporting Information Fig. S2A and S2B). PCA protected cell survival against OGD insult, but this action was lost when *Pkm2* was silenced (Fig. 3A). Ischemic injury was associated with oxidative stress, and PCA treatment effectively suppressed ROS generation in a PKM2-dependent manner (Fig. 3B). PCA protected mitochondrial function by preventing mitochondrial fragmentation and the opening of mitochondrial permeability transition pore (mPTP), but the protective effects were diminished by *Pkm2* knockdown (Fig. 3C and D). As a consequence, from the protection of mitochondrial integrity, PCA decreased the activity of caspase 3 (Fig. 3E). In addition, PCA treatment decreased the ratio of BAX/BCL-2 protein abundance and increased the inactivated caspase 3 by reducing the formation of cleaved caspase 3 in PKM2-dependent manner (Fig. 3F), and resultantly reduced cell apoptosis in a PKM2-dependent manner, indicated by the attenuated TUNEL

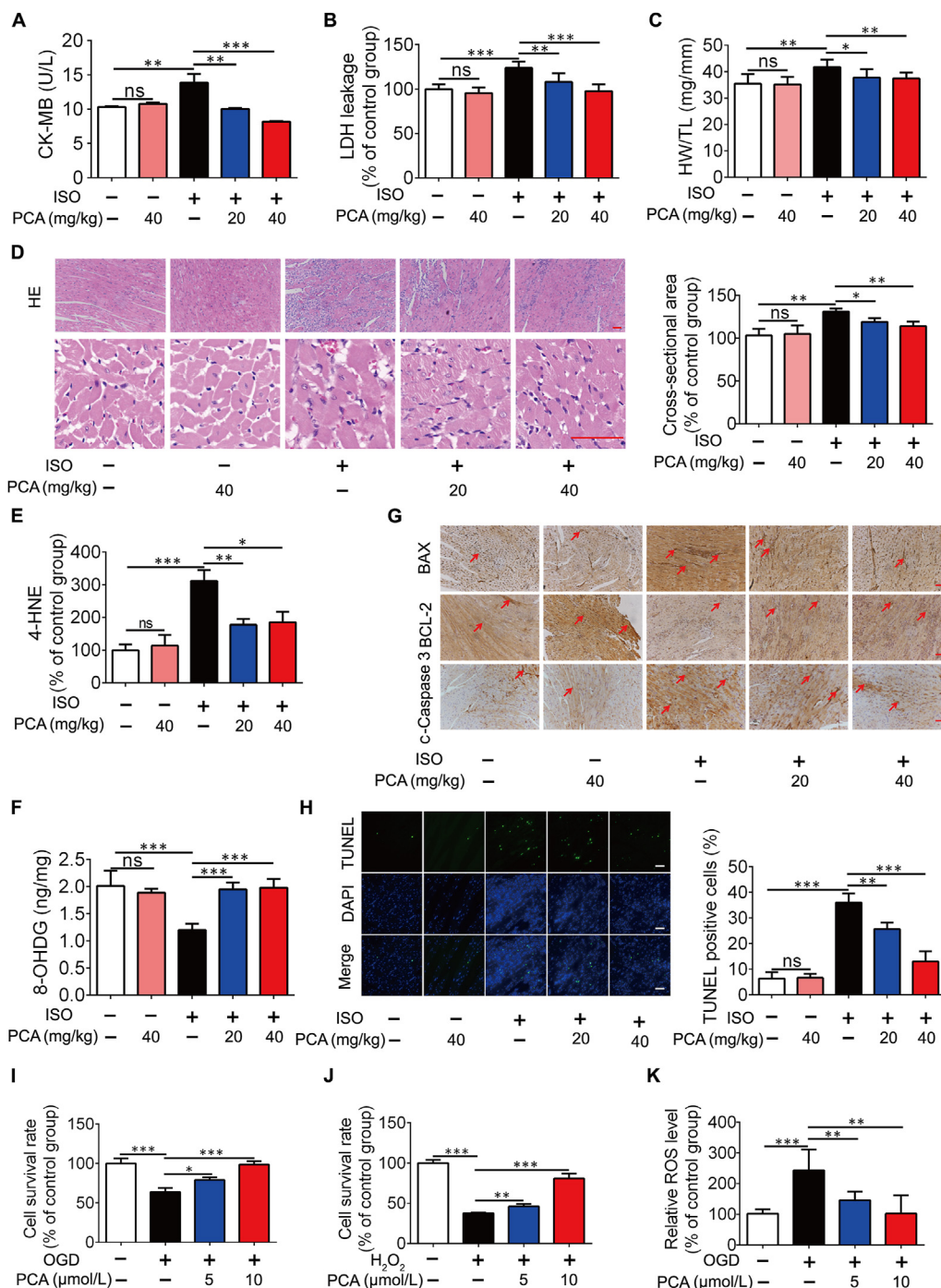


Figure 1 PCA protects the heart from ISO challenge in rats. The levels of circulating (A) CK-MB and (B) LDH in the plasma ($n = 6$). (C) The ratio of heart weight to tibia length (HW/TL) ($n = 6$). (D) One of representative H&E stained heart sections and cardiomyocyte cross-sectional area ($n = 6$, scale bar = 50 μ m). 4-HNE (E) and 8-OHDG (F) content in the heart ($n = 6$). (G) Immunocytochemical staining of BAX, BCL-2 and c-caspase 3 protein expression (one of 6 independent experiments; scale bar = 50 μ m). (H) Representative TUNEL staining images and quantification of TUNEL positive cells ($n = 6$). Cell survival of primary neonatal rat ventricular myocytes (NRVMs) when exposed to 1% O₂ in glucose-free DMEM (OGD) for 6 h (I) or H₂O₂ for 8 h (J) ($n = 6$). (K) Intracellular ROS production in NRVMs exposed to OGD for 4 h ($n = 6$). Results are shown as mean \pm SD; * $P < 0.05$, ** $P < 0.01$, *** $P < 0.001$.

staining (Fig. 3G). The anti-apoptotic effect was further confirmed by Annexin V-FITC detection (Fig. 3H). These results indicate that PKM2 is required for PCA to protect mitochondria to prevent cell apoptosis.

3.4. PCA promotes the nuclear localization of PKM2

To enact its metabolic enzyme activity, PKM2 resides in cytoplasm in the form of tetramer. When PKM2 is translocated to the

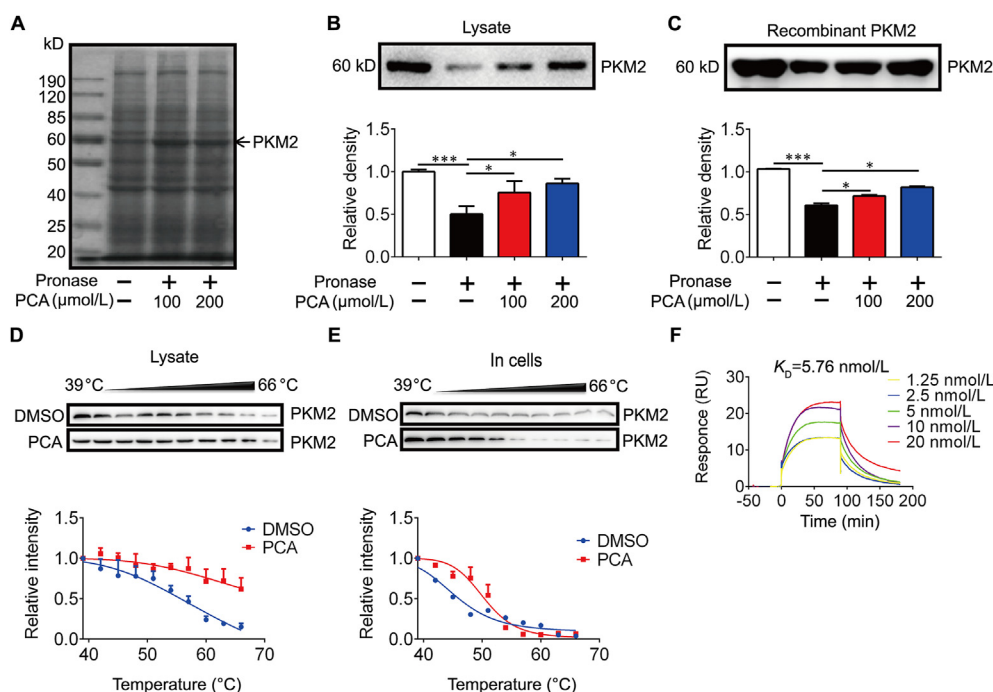


Figure 2 Identification of PKM2 as a direct binding target for PCA. (A) The employed drug affinity responsive target stabilization (DARTS) assay detects a marked increase in ~ 60 kD band upon PCA incubation in pronase digested H9C2 cell lysates. (B) Immunoblot analysis of PKM2 in pronase-digested cell lysate ($n = 3$). (C) Recombinant PKM2 in pronase-digested H9C2 cell lysates. PKM2 degradation in H9C2 cell lysates (D) and in intact cells (E) ($n = 3$). (F) Surface plasmon resonance (SPR) binding curve fit to a $K_d = 5.76$ nmol/L for PCA and PKM2 ($n = 3$). Results are shown as mean \pm SD; * $P < 0.05$, *** $P < 0.001$.

nuclear PKM2 in the form of dimer, its metabolic activity is reduced^{7,15}. Indeed, PKM2 activity was impaired by PCA in NRVMs (Fig. 4A). Therefore, we examined if PKM2 protects cardiomyocytes by regulating PKM2 shuttle between the cytosol and the nucleus. Although OGD induced PKM2 nuclear translocation, an adaptive response to rescue cell survival, the view of confocal microscopy and Western blot confirmed that PCA further potentiated the nuclear translocation. OGD insult could increase the expression of PKM2, PCA treatment further increase its nuclear localization (Fig. 4B–E). The shutting of PKM2 is influenced by acetylation modification, and SIRT6 promotes the nuclear export of PKM2 by deacetylation of PKM2 at Lys 433 residue^{34,35}. We conducted molecular docking analysis, and found that PCA is likely bind to a highly conserved residue Lys433 of PKM2 (Fig. 4F). In support, the result of immunoprecipitation showed that PCA treatment impaired the interaction between PKM2 and SIRT6 (Fig. 4G), partially explaining the preserved acetylation of PKM2 in cardiomyocytes (Fig. 4G). Once entering the nucleus, PKM2 interacts with β -catenin, and the formed complex is required for β -catenin transactivation⁷. As expected, PCA treatment increased the binding of β -catenin to PKM2 (Fig. 4H). Collectively, these results suggested that PCA disfavored PKM2-SIRT6 binding to retain PKM2 in the nucleus for β -catenin transactivation.

3.5. PCA upregulates survival genes through transactivation of β -catenin/TCF4

Since PKM2 is known as a β -catenin coactivator, we next asked whether the PCA influences β -catenin transactivation function via

regulation of PKM2. As β -catenin engages with TCF4 for transcriptional regulation of a variety of genes including *Myc*, *Ccnd1* and *Sgk1* that influence cell proliferation and apoptosis^{37,38}, we hypothesized that PCA might modulate the transcriptional activity of TCF4 dependent on a PKM2/ β -catenin/TCF4 signaling cascade. We found that the interaction of β -catenin and TCF4 was increased following PCA treatment in NRVMs exposed to OGD (Fig. 5A), and this action was also observed in cardiomyocytes when exposed to H₂O₂ (Fig. 5B). To investigate the downstream effect, we established a luciferase reporter gene assay for TCF4. PCA activated TCF4 transcription, but the action was blocked by PNU-74654, which binds to β -catenin to impair the interaction between β -catenin and TCF4 (Fig. 5C). *Myc*, *Ccnd1* and *Sgk1* are downstream genes targeted by TCF4, responsible for the regulation of cell survival^{6,37,38}. PCA upregulated these genes, but this action was impaired in the presence of PNU-74654 (Fig. 5D–F). Similarly, the protective effect of PCA on cell survival was also attenuated by co-treatment with PNU-74654 (Fig. 5G). These results provide evidence that PCA protected cardiomyocytes via regulating β -catenin and TCF4 signaling cascades.

3.6. PCA protects the heart against ischemic injury in a PKM2-dependent manner

To confirm PKM2-dependent role of PCA *in vivo*, we delivered an AAV9-expressing negative control (NC) or *Pkm2* shRNA fused with a *c-Tnt* promoter to induce heart-specific *Pkm2* KD in mice³⁶, and the efficiency was confirmed by detecting PKM2 and GFP tag by immunoblotting (Supporting Information Fig. S3A). We prepared LAD coronary artery ligation model in mice with

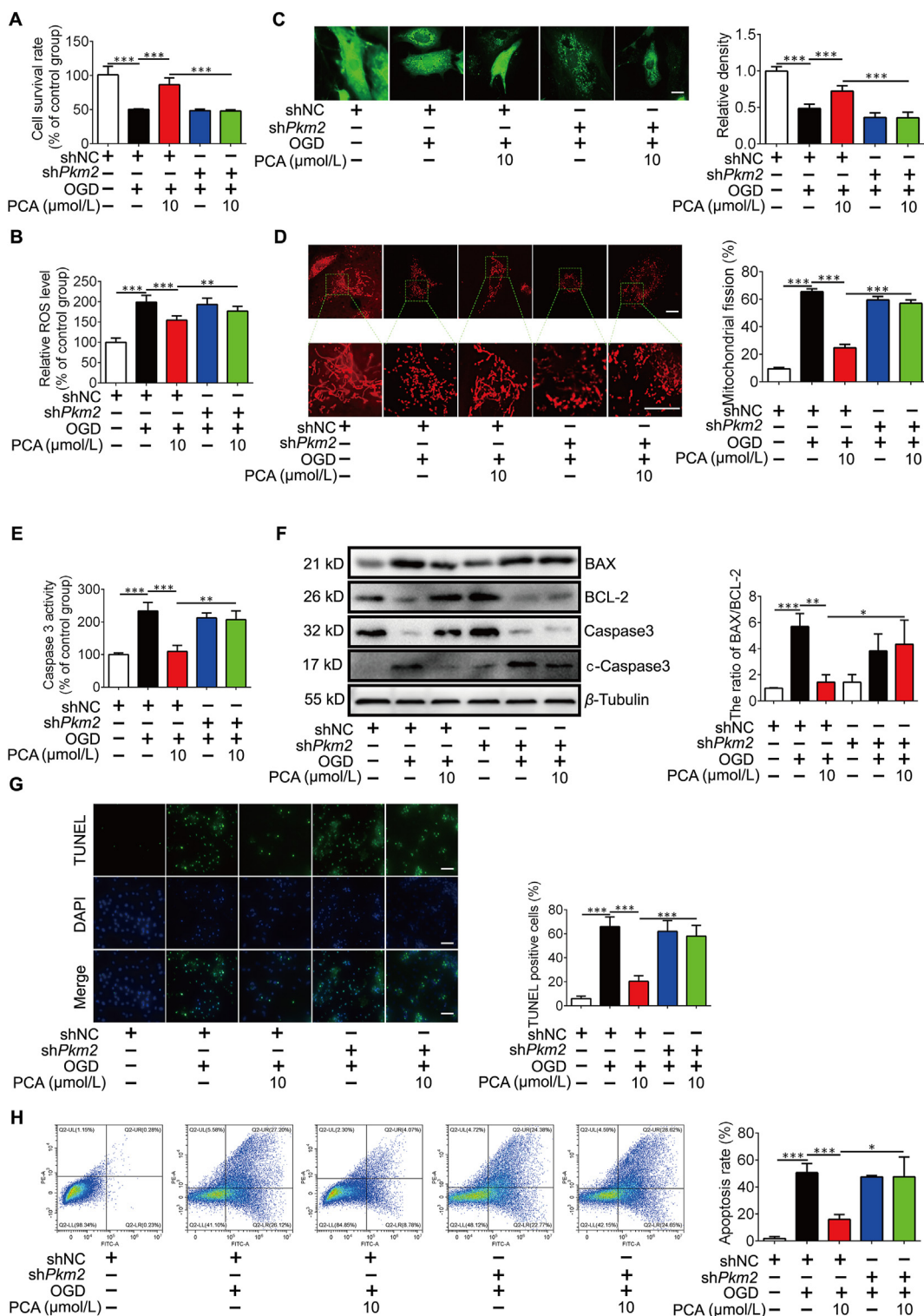


Figure 3 PCA PKM2-dependently protects cardiomyocytes. Primary neonatal rat ventricular myocytes (NRVMs) were cultured in glucose-free DMEM under 1% O_2 (OGD) for 4 h in the presence of protocatechuic aldehyde (PCA). (A) Cell survival in NRVMs exposed to OGD for 6 h ($n = 6$). (B) Intracellular ROS production ($n = 6$). (C) Representative images of mitochondrial permeability transition pore (mPTP) and quantification of relative fluorescence intensity ($n = 6$, one of three independent experiments). Scale bar: 10 μm . (D) Mitochondrial fission was detected by Mito-Tracker Red (one of 3 independent experiments) and quantification analysis. Scale bar: 10 μm . (E) Caspase 3 activity in NRVMs ($n = 6$). (F) Representative Western blots of BAX, BCL-2, caspase 3, cleaved caspase 3 (c-caspase 3) and the ratio of BAX/BCL-2 ($n = 3$). (G) Representative images of TUNEL staining and quantification analysis the percentage of apoptosis cells. Scale bars, 100 μm ($n = 3$). (H) Data of Annexin V/PI double staining flow cytometry; the percentage for each panel indicates the percentage of apoptotic cells and quantification of the percentage of apoptotic cells ($n = 3$). Results are shown as mean \pm SD; * $P < 0.05$, ** $P < 0.01$, *** $P < 0.001$.

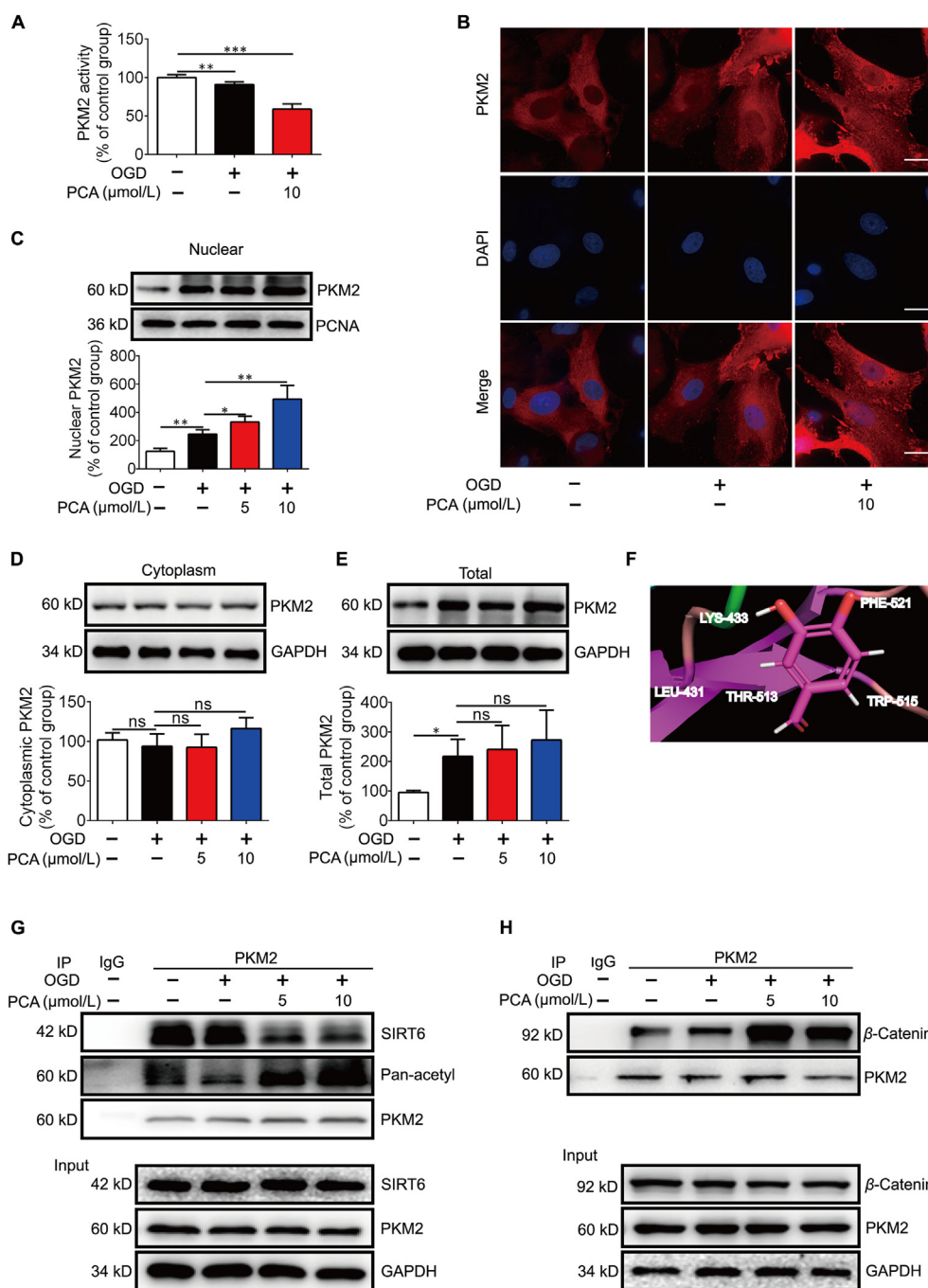


Figure 4 PCA promotes the nuclear localization of PKM2. Primary neonatal rat ventricular myocytes (NRVMs) were exposed to 1% O_2 in glucose-free DMEM (OGD) for 4 h in the presence of protocatechuic aldehyde (PCA). (A) PKM2 activity in NRVMs ($n = 6$). (B) Immunofluorescence image of endogenous PKM2 (one of three independent experiments. Scale bar: 10 μm). (C) Nuclear PKM2 protein expression ($n = 3$). (D) Cytoplasmic PKM2 protein expression ($n = 3$). (E) Total PKM2 protein expression ($n = 3$). (F) Docking analysis illustrates the interaction between PCA and PKM2. The residues that are likely to participate in the interactions with PCA are labeled. (G) Representative co-immunoprecipitation (co-IP) analysis of PKM2 and SIRT6 in the NRVMs ($n = 3$). (H) Representative co-IP of PKM2 and β -catenin in the NRVMs ($n = 3$). Results are shown as mean \pm SD; * $P < 0.05$, ** $P < 0.01$, *** $P < 0.001$.

PCA administration for 3 weeks (Fig. S3B). HE staining shows that ischemia led to heart injury, indicated by large area of cardiac infarct surface and broken fibers, but these abnormalities were attenuated by PCA administration in a manner dependent on PKM2 (Fig. 6A). Masson staining revealed that PCA reduced the deposition of extracellular matrix, but the role was lost in *Pkm2*-deficient heart (Fig. 6B). Consistently, PCA administration

reduced the contents 4-HNE in the heart (Fig. 6C). Echocardiography examination shows that PCA increased ejection fraction (EF) and fractional shortening (FS) in a manner dependent on cardiac PKM2 (Fig. 6D and E). Protein expression of PKM2 in the heart of adult mice is at a low level¹², but ischemia increased PKM2 protein expression as an adaptive response (Fig. 6F). Despite no significant influence on total PKM2 protein express,

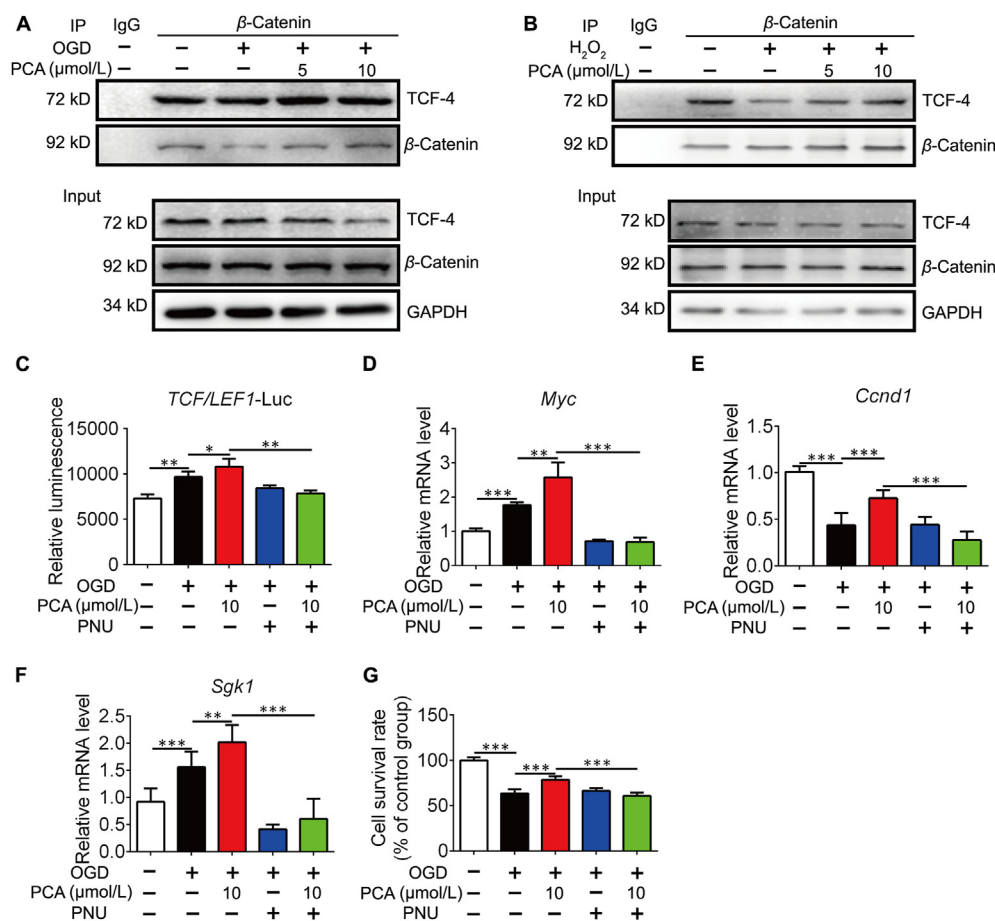


Figure 5 PCA regulates β -catenin/TCF4 cascades. Primary neonatal rat ventricular myocytes (NRVMs) were exposed to 1% O_2 in glucose-free DMEM (OGD) for 4 h in the presence of protocatechuic aldehyde (PCA). Representative co-IP analysis to of TCF4 and β -catenin in the NRVMs exposed to OGD for 4 h (A) or H_2O_2 for 8 h (B) ($n = 3$). (C) TCF4 luciferase reporter activity in the presence or absence of PNU-74654 (PUN, 10 μ mol/L) ($n = 3$). The mRNA levels of *Myc* (D), *Ccnd1* (E) and *Sgk1* (F) ($n = 4$). (G) Cell survival of NRVMs ($n = 6$). Results are shown as mean \pm SD; * $P < 0.05$, ** $P < 0.01$, *** $P < 0.001$.

PCA administration potentiated the binding of β -catenin to PKM2 and upregulated gene expression of *Myc*, *Ccnd1* and *Sgk1* dependently on PKM2 (Fig. 6F–I). Meanwhile, PCA reduced BAX and BCL-2 protein ratio, decrease the formation of cleaved caspase 3, resultantly reducing cell apoptosis in a PKM2-dependent manner (Fig. 6J). TUNEL staining was used to detect the apoptosis level of myocardial tissues and the result shows that the PCA treatment significantly decreased the TUNEL positive cells in the NC group, but not in the *Pkm2* KD group (Fig. 6K). PCA downregulated elevated levels of CK-MB and LDH in the blood, but the effects were lost in mice when heart *Pkm2* was deficient (Fig. S3C and S3D). These results provide evidence *in vivo* to support that PKM2 is required for PCA to protect the heart from ischemic injury.

4. Discussion

PKM2 regulates cell metabolism and growth under different conditions. Tumor cells and other rapidly growing cells mainly rely on aerobic glycolysis to meet metabolic demands and PKM2 shuttles into the nucleus as a co-activator for HIF-1 α transcription to support glycolysis³⁷. In the present study, we show that PCA promoted PKM2 nuclear translocation to rescue

cardiomyocyte survival from ischemic damage *via* regulation of β -catenin signaling cascades. PCA is reported to attenuate heart ischemic injury by restraining oxidative stress, endoplasmic reticulum stress and inflammatory response^{19,23,24}, and our finding provides another way from the aspect of transcriptional regulation. It is commonly proposed that nuclear PKM2/ β -catenin pathway regulates cell proliferation and tumor development, and we demonstrate that this regulation also confers the resistance of cardiomyocytes to cell death under nutrient deficient conditions.

ISO challenge induced heart damage, and we found that preventing mitochondrial apoptosis might be a way for PCA to rescue cell survival. More natural products have beneficial effects of cardioprotection, but it has been a challenging task for target discovery of underlying mechanisms. Chemical proteomics techniques have been used for this end^{41,42}, but a chemical probe that covalently links the ligand with targeted proteins is required to ensure further pull-down of the ligand-bound proteins for proteomic analysis. Nevertheless, for natural products that possess a relatively simple structure as PCA, any modification may distort the native ligand–protein interactions and jeopardize in assigning true binding proteins. Therefore, we employed a DARTS method for mapping the binding targets of PCA in hope to identify

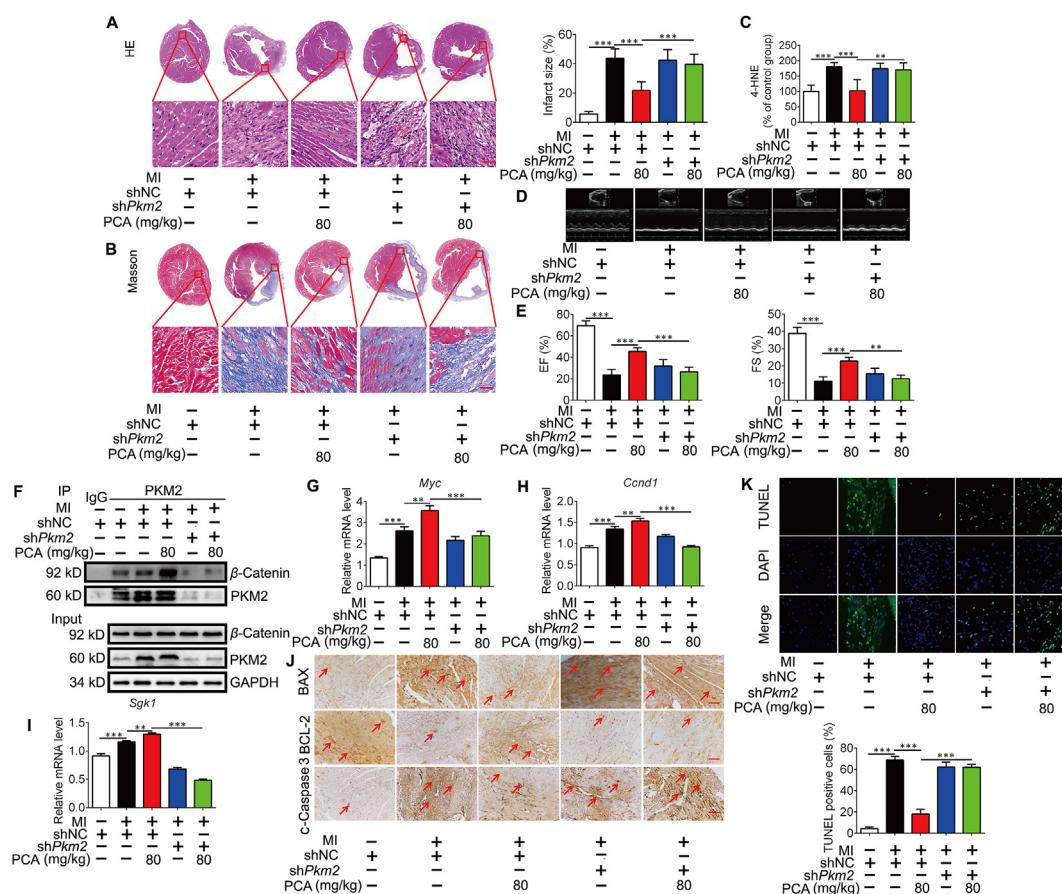


Figure 6 The myocardial protection effect of PCA is dependent on PKM2. Mice were orally administrated with protocatechuic aldehyde (PCA) for 3 weeks after coronary artery ligation. (A) Representative photomicrographs for HE staining of cardiac tissue sections ($n = 6$), Scale bar, 50 μm . (B) Representative photomicrographs for masson staining of cardiac tissue sections ($n = 6$). Scale bar, 50 μm . (C) 4-HNE contents in the heart ($n = 6$). (D) Representative M mode images of echocardiography from the assayed groups under treatments as indicated ($n = 6$). (E) Ejection fractions (EF) and shortening fraction (FS) in mice ($n = 6$). (F) Representative co-IP analysis of PKM2 and β -catenin in the heart ($n = 3$). The mRNA levels of *Myc* (G), *Cnd1* (H) and *Sgk1* (I) in the heart ($n = 6$). (J) Immunocytochemical staining of BAX, BCL-2 and c-caspase 3 protein expression ($n = 6$), scale bar = 50 μm . (K) Representative TUNEL staining images and quantification of TUNEL positive cells ($n = 6$). Results are shown as mean \pm SD; * $P < 0.05$, ** $P < 0.01$, *** $P < 0.001$.

proteins that are responsible for the PCA-mediated protective effect on cardiomyocytes under hypoxic conditions. DARTS provides a superior advantage compared to conventional chemical probe-based target discovery studies, since no modification is required to map the binding proteins for PCA. By visualizing the PCA-stabilized protein band on SDS-PAGE gels, we can identify the binding proteins and sought to investigate whether the identified target mediates cardioprotection of PCA.

In addition to the allosteric regulation, PKM2 subcellular location and functions are influenced by post-translational modifications⁶. For example, H_2O_2 decreased PKM2 enzymatic activity through oxidation of cysteine residue (Cys 358), which impairs the tetramer form³⁸. Oncogenic growth factors phosphorylate PKM2 at different residues to regulate its function and subcellular location differently⁶. SIRT6 is a member of sirtuin family of deacetylases involved in metabolic regulation. The lysine 433 residue of PKM2 is susceptible to acetylation regulation and SIRT6 mediates PKM2 nuclear export by deacetylation of PKM2 (Lys 433)^{34,35}. Because PCA blocked the interaction between SIRT6 and PKM2 in cardiomyocytes, it is rational to

believe that preserving PKM2 acetylation is a way for PCA to promote PKM2 translocation to the nucleus.

Although PKM2 is a key enzyme in glycolysis, accumulating evidence has highlighted the moonlighting functions of PKM2 when it enters the nucleus in different biological contexts. PKM2 is a low activity enzyme, whereas PKM1 is a constitutively active enzyme. Despite increased PKM2 induction, total pyruvate kinase activity is still reduced in ischemic heart¹⁰. In pulmonary arterial smooth muscle cells, hypoxia is also shown to reduce PK activity³⁹. When PKM2 is translocated to the nucleus, PKM2 acts as co-factor for transcriptional regulation, its metabolic activity is reduced^{7,15}. PCA promotes PKM2 nuclear import, and the formation of PKM2 dimer and nuclear location should be the reason for the reduced PKM2 metabolic activity. When PKM2 is translocated into the nucleus, PKM1 is predicted to maintain the enzymatic activity.

In cancer cells nuclear PKM2 has both protein kinase and transcription co-activator functions^{13,40}. For instance, by acting as a protein kinase in the nucleus, PKM2 directly binds and phosphorylates histone H3, consequently inducing tumor cell

proliferation and cell cycle progression *via* transcriptional regulation of *Ccnd1* and *Myc*¹⁵. As a transcriptional co-activator, PKM2 binds to β -catenin and directly regulates cell cycle progression through controlling cyclin D1 expression^{7,37}. The role of PKM2 in heart is revealed by a recent study which shows that PKM2 elongates cell survival and improves cardiac function in ischemic heart through β -catenin¹². WNT/ β -catenin signaling in cell proliferation and tumorigenesis has been well-documented, recent studies demonstrate the potential role of β -catenin in the protection of cardiomyocytes, especially in the setting of ischemic injury^{12,18,41}. In cardiomyocytes, PCA promoted PKM2 translocation into the nucleus with the association of β -catenin. Together with TCF4 induction, β -catenin upregulates gene induction of *Myc*, *Ccnd1* and *Sgk1* to exert anti-apoptotic effects. Cyclin D1 (encoded by *Ccnd1* gene) is a key regulator of cell proliferation, increasing resistance to apoptosis⁴². SGK1 encodes the protein of serine/threonine kinase family, and protects cell survival from oxidative stress⁴³. c-Myc (encoded by *Myc* gene) regulates cell proliferation with inhibition of apoptosis⁴⁴. Because these genes are regulated by β -catenin/TCF4 signaling under stress conditions, we reason that the induction of these genes by PCA has a contribution to protecting cardiomyocytes from apoptosis under ischemic conditions.

Because ischemia-induced myocardial infarction and necrosis are nearly irreversible, the protective effects of PCA were investigated using a coronary artery ligation mice model with a long-term administration (3 weeks after surgery). In addition, PCA improved heart contractive function and rescued cell survival from apoptosis in a PKM2-dependent manner, because PCA increased the interaction between PKM2 and β -catenin in the heart. PKM2 induction is also observed in failing heart with enhanced aerobic glycolysis, as glucose oxidation was impaired due to phosphoinositide-dependent kinase (PDK) induction⁴⁵. PKM2 induction provides metabolic support to cardiac hypertrophy *via* transcriptional activation of proliferation-associated target genes, responsible for impaired heart function⁴⁶. These events indicate that PKM2 plays the role differently under different pathological conditions. Therefore, we should note that regulation of nuclear PKM2 by PCA is in the setting of ischemic injury. PCA administration attenuates cardiac fibrosis, but we cannot say with certainty that this action is a result from direct regulation of PKM2. Although aerobic glycolysis is regarded as a hallmark of tumor metabolism, emerging evidence indicates that augmented glycolysis and PKM2 induction are associated with myofibroblast activation due to metabolic reprogramming^{47,48}. PKM2 dimer, rather than the tetramer, induces fibroblast activation, suggesting the potential role of nuclear PKM2 in fibrotic response⁴⁷. Because fibrosis is a response for the replacement of dead cells, we reason that cardiomyocyte protection by PKM2 has a contribution to attenuating fibrotic response after myocardial infarction.

Although PCA regulates PKM2/ β -catenin signaling cascades to protect cardiomyocytes from ischemic injury, this conclusion is not exclusive, because more pathological factors converge in the injury. PCA is a multifunctional product and can protect the heart from different mechanisms. Although accumulating evidence demonstrates the beneficial effects of PCA on cardioprotection^{18,46,47}, some studies suggested the potential pathophysiological risks associated with its metabolism^{48,49}. Therefore, a comprehensive study considering its metabolic and pharmacokinetic changes and potential toxicity is needed for its practical application in the management of cardiovascular diseases.

5. Conclusions

Our study has designated PCA as a natural product that promoted PKM2 translocation to the nucleus through direct engagement. Under ischemic conditions, the nuclear PKM2 initiated β -catenin/TCF4 signaling cascades and mediated relative gene induction involved in the regulation of cell survival, having a contribution to rescuing cardiomyocytes from mitochondrial apoptosis. Our finding suggests that regulation of PKM2/ β -catenin/TCF4 signaling is a way to combat ischemic heart injury.

Acknowledgments

This work was supported by the National Key R&D Program of China (2019YFC1711000), the National Natural Science Foundation of China (81421005 and 81722048), “Double First-Class” University project (CPU2018GF04 and CPU2018GY09, China). We thank the platform support of the State Key Laboratory of Natural Medicines.

Author contributions

Xunxun Wu, Lian Liu, Qiuling Zheng and Hui Ye performed the research. Xunxun Wu, Lian Liu and Hui Ye wrote the original draft. Haiping Hao critically reviewed the paper. Hua Yang, Ping Li and Hui Ye conceived the project, supervised research and critically reviewed the paper.

Conflicts of interest

The authors declare no conflicts of interest.

Appendix A. Supporting information

Supporting data to this article can be found online at <https://doi.org/10.1016/j.apsb.2021.03.021>.

References

- Cheng Y, Feng Y, Xia Z, Li X, Rong J. ω -Alkynyl arachidonic acid promotes anti-inflammatory macrophage M2 polarization against acute myocardial infarction *via* regulating the cross-talk between PKM2, HIF-1 α and iNOS. *Biochim Biophys Acta Mol Cell Biol Lipids* 2017;**1862**:1595–605.
- Wang J, Zhou H. Mitochondrial quality control mechanisms as molecular targets in cardiac ischemia–reperfusion injury. *Acta Pharm Sin B* 2020;**10**:1866–79.
- Hsieh PCH, Segers VFM, Davis ME, MacGillivray C, Gannon J, Molkenin JD, et al. Evidence from a genetic fate-mapping study that stem cells refresh adult mammalian cardiomyocytes after injury. *Nat Med* 2007;**13**:970–4.
- Senyo SE, Steinhilber ML, Pizzimenti CL, Yang VK, Cai L, Wang M, et al. Mammalian heart renewal by pre-existing cardiomyocytes. *Nature* 2013;**493**:433–6.
- Chen CY, Choong OK, Liu LW, Cheng YC, Li SC, Yen CYT, et al. MicroRNA let-7-TGFB3 signalling regulates cardiomyocyte apoptosis after infarction. *EBioMedicine* 2019;**46**:236–47.
- Alquraishi M, Puckett DL, Alani DS, Humidat AS, Frankel VD, Donohoe DR, et al. Pyruvate kinase M2: a simple molecule with complex functions. *Free Radic Biol Med* 2019;**143**:176–92.
- Yang W, Xia Y, Ji H, Zheng Y, Liang J, Huang W, et al. Nuclear PKM2 regulates β -catenin transactivation upon EGFR activation. *Nature* 2011;**480**:118–22.

8. Azoitei N, Becher A, Steinestel K, Rouhi A, Diepold K, Genze F, et al. PKM2 promotes tumor angiogenesis by regulating HIF-1 α through NF- κ B activation. *Mol Cancer* 2016;**15**:3.
9. Li Q, Qi X, Jia W. 3,3',5-Triiodothyroxine inhibits apoptosis and oxidative stress by the PKM2/PKM1 ratio during oxygen-glucose deprivation/reperfusion AC16 and HCM-a cells: T3 inhibits apoptosis and oxidative stress by PKM2/PKM1 ratio. *Biochem Biophys Res Commun* 2016;**475**:51–6.
10. Williams AL, Khadka V, Tang M, Avelar A, Schunke KJ, Menor M, et al. HIF1 mediates a switch in pyruvate kinase isoforms after myocardial infarction. *Physiol Genom* 2018;**50**:479–94.
11. Shi J, Yang X, Yang D, Li Y, Liu Y. Pyruvate kinase isoenzyme M2 expression correlates with survival of cardiomyocytes after allogeneic rat heterotopic heart transplantation. *Pathol Res Pract* 2015;**211**:12–9.
12. Magadam A, Singh N, Kurian AA, Munir I, Mehmood T, Brown K, et al. Pkm 2 regulates cardiomyocyte cell cycle and promotes cardiac regeneration. *Circulation* 2020;**141**:1249–65.
13. Gao X, Wang H, Yang JJ, Liu X, Liu ZR. Pyruvate kinase M2 regulates gene transcription by acting as a protein kinase. *Mol Cell* 2012;**45**:598–609.
14. Jiang Y, Wang Y, Wang T, Hawke DH, Zheng Y, Li X, et al. PKM2 phosphorylates MLC2 and regulates cytokinesis of tumour cells. *Nat Commun* 2014;**5**:5566.
15. Yang W, Xia Y, Hawke D, Li X, Liang J, Xing D, et al. PKM2 phosphorylates histone H3 and promotes gene transcription and tumorigenesis. *Cell* 2012;**150**:685–96.
16. Valenta T, Hausmann G, Basler K. The many faces and functions of β -catenin. *EMBO J* 2012;**31**:2714–36.
17. Hahn JY, Cho HJ, Bae JW, Yuk HS, Kim KI, Park KW, et al. Beta-catenin overexpression reduces myocardial infarct size through differential effects on cardiomyocytes and cardiac fibroblasts. *J Biol Chem* 2006;**281**:30979–89.
18. Ying Y, Zhu H, Liang Z, Ma X, Li S. GLP1 protects cardiomyocytes from palmitate-induced apoptosis via Akt/GSK3 β / β -catenin pathway. *J Mol Endocrinol* 2015;**55**:245–62.
19. Jiang L, Zeng H, Ni L, Qi L, Xu Y, Xia L, et al. HIF-1 α preconditioning potentiates antioxidant activity in ischemic injury: the role of sequential administration of dihydrotanshinone I and protocatechuic aldehyde in cardioprotection. *Antioxidants Redox Signal* 2019;**31**:227–42.
20. Zeng H, Wang L, Zhang J, Pan T, Yu Y, Lu J, et al. Activated PKB/GSK-3 β synergizes with PKC- δ signaling in attenuating myocardial ischemia/reperfusion injury via potentiation of NRF2 activity: therapeutic efficacy of dihydrotanshinone-I. *Acta Pharm Sin B* 2021;**11**:71–88.
21. Gao L, Wu WF, Dong L, Ren GL, Li HD, Yang Q, et al. Protocatechuic aldehyde attenuates cisplatin-induced acute kidney injury by suppressing nox-mediated oxidative stress and renal inflammation. *Front Pharmacol* 2016;**7**:479.
22. Gay NH, Phopin K, Suwanjang W, Songtawee N, Ruankham W, Wongchitrat P, et al. Neuroprotective effects of phenolic and carboxylic acids on oxidative stress-induced toxicity in human neuroblastoma SH-SY5Y cells. *Neurochem Res* 2018;**43**:619–36.
23. Guo C, Wang S, Duan J, Jia N, Zhu Y, Ding Y, et al. Protocatechuic aldehyde protects against cerebral ischemia-reperfusion-induced oxidative injury via protein kinase Ce/Nrf 2/HO-1 pathway. *Mol Neurobiol* 2017;**54**:833–45.
24. Zhou Z, Liu Y, Miao AD, Wang SQ. Protocatechuic aldehyde suppresses TNF- α -induced ICAM-1 and VCAM-1 expression in human umbilical vein endothelial cells. *Eur J Pharmacol* 2005;**513**:1–8.
25. Xing YL, Zhou Z, Agula, Zhong ZY, Ma YJ, Zhao YL, et al. Protocatechuic aldehyde inhibits lipopolysaccharide-induced human umbilical vein endothelial cell apoptosis via regulation of caspase-3. *Phytother Res* 2012;**26**:1334–41.
26. Moon CY, Ku CR, Cho YH, Lee EJ. Protocatechuic aldehyde inhibits migration and proliferation of vascular smooth muscle cells and intravascular thrombosis. *Biochem Biophys Res Commun* 2012;**423**:116–21.
27. Zhang L, Wei TT, Li Y, Li J, Fan Y, Huang FQ, et al. Functional metabolomics characterizes a key role for acetylneuraminic acid in coronary artery diseases. *Circulation* 2018;**137**:1374–90.
28. Li Q, Cao L, Tian Y, Zhang P, Ding C, Lu W, et al. Butyrate suppresses the proliferation of colorectal cancer cells via targeting pyruvate kinase M2 and metabolic reprogramming. *Mol Cell Proteomics* 2018;**17**:1531–45.
29. Lomenick B, Hao R, Jonai N, Chin RM, Aghajan M, Warburton S, et al. Target identification using drug affinity responsive target stability (DARTS). *Proc Natl Acad Sci U S A* 2009;**106**:21984–9.
30. Wang LC, Liao LX, Lv HN, Liu D, Dong W, Zhu J, et al. Highly selective activation of heat shock protein 70 by allosteric regulation provides an insight into efficient neuroinflammation inhibition. *EBioMedicine* 2017;**23**:160–72.
31. Zhao H, Caffisch A. Discovery of dual ZAP70 and Syk kinases inhibitors by docking into a rare C-helix-out conformation of Syk. *Bioorg Med Chem Lett* 2014;**24**:1523–7.
32. Garg M, Khanna D. Exploration of pharmacological interventions to prevent isoproterenol-induced myocardial infarction in experimental models. *Ther Adv Cardiovasc Dis* 2014;**8**:155–69.
33. Lomenick B, Jung G, Wohlschlegel JA, Huang J. Target identification using drug affinity responsive target stability (DARTS). *Curr Protoc Chem Biol* 2011;**3**:163–80.
34. Lv L, Xu YP, Zhao D, Li FL, Wang W, Sasaki N, et al. Mitogenic and oncogenic stimulation of K433 acetylation promotes PKM2 protein kinase activity and nuclear localization. *Mol Cell* 2013;**52**:340–52.
35. Bhardwaj A, Das S. SIRT6 deacetylates PKM2 to suppress its nuclear localization and oncogenic functions. *Proc Natl Acad Sci U S A* 2016;**113**:E538–47.
36. Werfel S, Jungmann A, Lehmann L, Ksienzyk J, Bekeredjian R, Kaya Z, et al. Rapid and highly efficient inducible cardiac gene knockout in adult mice using AAV-mediated expression of Cre recombinase. *Cardiovasc Res* 2014;**104**:15–23.
37. Luo W, Hu H, Chang R, Zhong J, Knabel M, O'Meally R, et al. Pyruvate kinase M2 is a PHD3-stimulated coactivator for hypoxia-inducible factor 1. *Cell* 2011;**145**:732–44.
38. Anastasiou D, Pouligiannis G, Asara JM, Boxer MB, Jiang Jk, Shen M, et al. Inhibition of pyruvate kinase M2 by reactive oxygen species contributes to cellular antioxidant responses. *Science* 2011;**334**:1278–83.
39. Guo D, Gu J, Jiang H, Ahmed A, Zhang Z, Gu Y. Inhibition of pyruvate kinase M2 by reactive oxygen species contributes to the development of pulmonary arterial hypertension. *J Mol Cell Cardiol* 2016;**91**:179–87.
40. Chen D, Wei L, Liu ZR, Yang JJ, Gu X, Wei ZZ, et al. Pyruvate kinase M2 increases angiogenesis, neurogenesis, and functional recovery mediated by upregulation of STAT3 and focal adhesion kinase activities after ischemic stroke in adult mice. *Neurotherapeutics* 2018;**15**:770–84.
41. Fan Y, Ho BX, Pang JKS, Pek NMQ, Hor JH, Ng SY, et al. Wnt/ β -catenin-mediated signaling re-activates proliferation of matured cardiomyocytes. *Stem Cell Res Ther* 2018;**9**:338.
42. Roué G, Pichereau V, Lincet H, Colomer D, Sola B. Cyclin D1 mediates resistance to apoptosis through upregulation of molecular chaperones and consequent redistribution of cell death regulators. *Oncogene* 2008;**27**:4909–20.
43. Schoenebeck B, Bader V, Zhu XR, Schmitz B, Lübbert H, Stichel CC. Sgk1, a cell survival response in neurodegenerative diseases. *Mol Cell Neurosci* 2005;**30**:249–64.
44. Thompson EB. The many roles of c-Myc in apoptosis. *Annu Rev Physiol* 1998;**60**:575–600.

45. Rees ML, Subramaniam J, Li Y, Hamilton DJ, Frazier OH, Taegtmeyer H. A PKM2 signature in the failing heart. *Biochem Biophys Res Commun* 2015;**459**:430–6.
46. Hauck L, Dadson K, Chauhan S, Grothe D, Billia F. Inhibiting the Pkm 2/b-catenin axis drives *in vivo* replication of adult cardiomyocytes following experimental MI. *Cell Death Differ* 2020;**28**:1398–417.
47. Zheng D, Jiang Y, Qu C, Yuan H, Hu K, He L, et al. Pyruvate kinase M2 tetramerization protects against hepatic stellate cell activation and liver fibrosis. *Am J Pathol* 2020;**190**:2267–81.
48. Xie N, Tan Z, Banerjee S, Cui H, Ge J, Liu RM, et al. Glycolytic reprogramming in myofibroblast differentiation and lung fibrosis. *Am J Respir Crit Care Med* 2015;**192**:1462–74.